Investigation of Cr (VI) adsorption from aqueous media by using synthetic chitosan-allophane nanocomposite adsorbent: characteristics, kinetic and isotherm

Hosein Pazoki
Iran University of Science and Technology

Mansoor Anbia
anbia@iust.ac.r

Iran University of Science and Technology

Additional Declarations: No competing interests reported.

Abstract

This study investigates Cr (VI) removal from aqueous solution by synthetic chitosan-allophane nanocomposite. The nanocomposite was synthesized in the solvothermal method. The adsorbent was characterized utilizing X-ray diffraction (XRD), Fourier transforms infrared (FT-IR), Scanning electron microscope (SEM) image and Brunauer-Emmet-Teller (BET) method. This work investigated of influence of solid/liquid ratio, pH, contact time, initial concertation on the adsorption process, adsorption kinetics, and isotherms. The maximum adsorption capacity of synthetic nanocomposite for Cr (VI) is 112.17 (mg/g) on optimum conditions. The kinetics study shows that the pseudo-second-order kinetic equation better describes adsorbents' adsorption behavior. The isotherms study suggests that the adsorption process of synthetic chitosan-allophane nanocomposite follow the Langmuir model. Moreover, the stability and reproducibility of synthetic nano composite were investigated.

Introduction

In recent decades, the widespread industrial activities and technological advancements have led to the release of various pollutants into the environment, posing significant threats to both ecosystems and human health [1] .Chromium, in its hexavalent state (Cr (VI)) which widely used in diverse industrial processes such as metal plating, leather tanning, and textile manufacturing, is one such harmful pollutants for its toxicity and adverse effects on human health and ecosystems. As industrial activities continue to expand, the discharge of Cr(VI) into water bodies has also increased that is required to effective and sustainable remediation strategies. [2,3]. The conventional methods such as chemical precipitation [4], membrane filtration [5], biological methods [6], electrochemical methods and ion exchange [7] have been widely employed for chromium removal. Despite the progress made in Cr (VI) removal methods, these methods often have limitations such as including cost-effectiveness, scalability, and environmental impact. Future research directions may focus on developing integrated and sustainable approaches to improve these challenges [8]. The absorption method for ion removal is found a highly effective and versatile technique in water treatment processes. Because it exhibits high efficiency, ensuring a rapid and thorough removal of ions from the solution. Its scalability and adaptability make it suitable for both small-scale applications and large-scale industrial processes [9,10]. Moreover, the method is known for its cost-effectiveness, because many absorbent materials can be regenerated and reused, minimizing operational expenses [11]. Furthermore, the absorption process is environmentally friendly, particularly when using eco-friendly absorbents, contributing to sustainable practices in ion removal [12]. Allophane is amorphous aluminosilicate that exists both naturally and synthetically, and is suitable in the efficient removal of ions from various environments [13]. One of convenient features is their exceptional ion-exchange capacity, allowing for efficient and selective removal of ions from aqueous solutions [14]. Their high surface area, high degree of chemical stability and unique structure provide numerous active sites for ion adsorption, enhancing the overall effectiveness of the removal process [15]. Allophanes are produced often naturally occurring minerals or synthetically that it causes very little adverse effects on the environment which contribute to their environmentally friendly nature. The adaptability of allophanes in targeting a wide range of ions, together with their low cost and sustainability, have made them known as promising and advantageous adsorbents for ion removal from wastewater in absorption processes [16–18]. Chitosan, a biodegradable and non-toxic biopolymer derived from chitin which used as an adsorbent in recent years due to its remarkable properties such as: biocompatibility, adsorption capabilities, unique chemical structure, versatile functional group and eco-friendly nature [19,20]. The chemical structure of chitosan includes amino and hydroxyl groups, provides a proper active site for interaction with various contaminants that created an effective sorbent for pollutants including: heavy metals, dyes, and organic compounds in absorption processes [21,22]. Additionally, its cost-effectiveness and ease of modification, caused it as a promising candidate for wastewater treatment [23]. The nano chitosan due to its suitable properties that includes self-assembly, large surface area and enhanced reactivity is known as good candidate for water treatment [24]. In order to for preparation of nano chitosan have been developed different method which involves polyelectrolyte complexation [25], ionic gelation, desolvation [26], emulsion crosslinking, spray-drying, emulsion droplet coalescence [27], and reverse micellar method [28]. The modification of adsorbents has been used by physical and chemical methods that develop their properties such as: pore size, mechanical strength, chemical stability, hydrophilicity, adsorption capacity and also biocompatibility [29]. The incorporate allophane with nano chitosan to composite materials presents an improved adsorbent with enhanced mechanical, thermal, and antimicrobial properties [30]. In this study, first, we synthesis an allophane adsorbent through green hydrothermal method then preparation of nano chitosan in order to composite with allophane, thoroughly characterizing its textural, structural, and morphological properties. Subsequently, we applied the adsorbent in batch adsorption processes to remove Cr (VI) toxic metal ions from aqueous solutions. The operational parameters were investigated and optimized to understand influence of pH, initial nitrate concentration, adsorbent dosage and contact time on the removal of Cr (VI) ions from

aqueous solution. Also, the bath adsorption isotherms and kinetic were comprehensively explored. This study introduces a novel approach to synthesizing high surface area, reusable, and stable adsorbent for effectively adsorbing hard metal ions from wastewaters, contributing to environmental remediation.

Materials and methods

Materials

Chitosan with 85% deacetylated and sodium metasilicate (Na_2SiO_3) were acquired from Sigma-Aldrich. The crosslinking agent TPP and the solvent glacial acetic acid, ethanol (96 wt %), hydrochloric acid (HCl) (37 wt %), sodium hydroxide (NaOH) (99 wt %), potassium dichromate ($K_2Cr_2O_7$) (99 wt %) and aluminum chloride ($AlCl_3$) (99 wt %) were procured from Merck.

Synthesis of allophane

In order to synthesize allophane, first 2.9 grams of aluminum chloride with 1.2 grams of sodium metasilicate dissolve in 100 ml of water, then slowly add sodium hydroxide solution (2 M) dropwise to the previous mixture until the pH should be around 6 to 7. Finally, the present solution was transferred to a teflon autoclave and placed in an oven with a temperature of 150°C for 48 hours. Then the resulting white precipitate was washed with distilled water and dried in an oven at 80°C.

Preparation of allophane-chitosan nanocomposites

The Ionotropic gelation technique used to preparation of allophane-chitosan nanocomposites. In order to preparation of nanocomposites 0.6 g of chitosan dissolved in 80 mL of acetic acid 2% (V/V). After preparing a homogeneous viscous solution, 4.12 g of TPP dissolved in 115 mL of deionized water was then added in drop wise with rapid stirring for a period of 20 min, a milky emulsion was obtained which is the nano chitosan. In the following, 0.6 g allophane added into previous solution is stirring for 4 h at 25°C. A precipitate was recovered by filtration and washed with deionized water and dried in a freeze dryer for 24 h.

Characterization

Various conventional techniques were employed to characterize the mordenite sample. X-ray diffraction (XRD) analysis was conducted to characterize the synthesized crystalline clinoptilolite zeolite. The XRD patterns were obtained using a Philips 1830 diffractometer with Cu-Kα radiation, operating at 40 kV and 20 mA. Surface analysis, including surface area, pore size diameter, and pore volume, was carried out using nitrogen adsorption on a Micromeritics model ASAP 2020 analyzer. Quantitative analysis of the species was performed through inductively coupled plasma atomic emission spectrometry (ICP-AES) using a S7000 instrument from SHIMADZU. The Fourier transform infrared (FT-IR) spectrum of the adsorbent was recorded at room temperature on a DIGILAB FTS 7000 spectrometer equipped with an attenuated total reflection (ATR) cell. Morphological properties were investigated using a scanning electron microscope (SEM) (PHILIPS XL30).

Cr (VI)adsorption experiments

The experiment involving the batch adsorption of Cr (VI) metal ion synthetic chitosan-allophane nanocomposite adsorbent was conducted at 25°C using a batch method with varying initial concentrations. To reach equilibrium, a mixture of adsorbent and metal ion solution was stirred at a constant rotation speed of 150 rpm and a consistent temperature. Residual metal ion concentrations in the samples were measured using ICP-AES. The kinetics of sorption were examined at an initial metal concentration of 100 mg/L in a 50 mL and 25°C. Additionally, the equilibrium adsorption capacity (q_e, mg/g), the adsorption capacity at different time points (q_t, mg/g), and the percentage of metal ion adsorption (R%) were calculated as follows:

$q_e = (C_0-C_e)$ V/m (1)

$q_t = (C_0-C_t)$ V/m (2)

R% = $(C_0-C_e) / C_e$ (3)

where C_0 is the initial concentration of metal ions (mg/L), C_e is the final concentration of metal ions (mg/L), C_t is the concentration of metal ions at time t (mg/L), V is the volume of the aqueous (L) and m is the adsorbent mass (g).

.

Results and discussion

The N_2 adsorption–desorption analysis

The N_2 isotherms of prepared allophane, nano chitosan and allophane-chitosan nanocomposites are indicated in Fig. 1a-c, respectively. The structure properties of compounds such as surface area, pore volumes and pore size diameter were obtained using the Brunauer–Emmett–Teller (BET) method and the BJH method. The results obtained from the nitrogen adsorption/desorption analysis are revealed in Table 1. The isotherms of compounds exhibit a type of II. The based on the average pore size, the pore can fall into three categories: micropores are defined as pores with diameter not exceeding 2 nm, mesopores are pores with diameters between 2 and 50 nm and macropores represent pores with diameter larger than 50 nm [31]. The BET specific surface area of allophane, nano-chitosan and allophane-chitosan nanocomposite is 296.52, 40.98 and 222.37 m^2/g, respectively. As is clear the BET surface area and pore volume of allophane-chitosan nanocomposite is lower compared to allophane which a possible reason is due to partial occupation of pore of allophane with chitosan nanoparticle by hydrogen bonding. The higher functionalized groups on the surface area enhanced accessibility of reactant sites to achieve better performance in adsorption processes [32]. Furthermore, the overall structure of allophane-chitosan nanocomposite has not changed much.

Table 1
Textural properties determined from nitrogen adsorption–desorption experiments.

Sample	S_{BET} ($m^2.g^{-1}$)	Pore volume ($cm^3. g^{-1}$)	Pore diameter (nm)
Allophane	296.52	0.4507	4.47
Nano chitosan	40.98	0.09	9.24
Chitosan-allophane nanocomposite	222.37	0.1798	0.31

FT-IR spectra analysis

The adsorption wavenumber of synthetic allophane in FT-IR spectrum including 3448, 1635, 1033, 910, 532,439, and 316 cm^{-1} that are presented in Fig. 1d. The peak of hydroxyl groups is appeared about 3448 cm^{-1} which related to silanol or aluminol. The stretching of the OH hydroxyl group is presented in the range 3800 – 3000 cm^{-1}. The existence of the Si-O-Si vibration bond in the structure of the compound can be seen in range 1000 cm-1–1100 cm^{-1}. The absorption peak of Si-O-Si is indicated in wave number 1033.85 cm^{-1}. The absorption peak at about 1635 cm^{-1} is related to bonding water molecular. The stretching bond of Si-O-Al of aluminosilicate is shown at about 910.40 cm^{-1}. The absorption peak at about 532 cm^{-1} is appeared which it shows existence of Al octahedral. This study was obtained the peak adsorption that have been reported in previous researchers [16]. In the FT-IR spectrum of nano chitosan (Fig. 1e) the broad peak adsorption 3500 to 3200 cm^{-1} is related to the tensile vibration of the OH group and the N-H group. The $-NH_2$ absorption peak is indicated at 1596 cm^{-1}. The presence of two adsorption peak at 1541 cm^{-1} and 1647 cm^{-1} are duo to the N-H bending vibration of protonated amino ($-NH_2$) group and C-H bending vibration of the alkyl group. The asymmetric stretching vibrations P-O-P and stretching P-O bonds were indicated at about 889 and 1226 cm^{-1}. The adsorption peak at about 1070 cm^{-1} was attributed to C-O-C stretching vibration bond which is similar results by other researchers [33]. The FT-IR spectrum of chitosan-allophane nanocomposite is shown in Fig. 1f. It can be seen the spectrum of nanocomposite does not change much with allophane, only the peaks have become wider, which is due to the hydrogen bonding. So, this observation confirms that the combination of allophane and nano chitosan has done [34].

XRD patterns of adsorbent

The location of peaks at 2θ at 26.2°, 40.1° and 66.2° are displayed in Fig. 1g which related to peaks of synthetic of allophane. As can be seen the XRD pattern does not contain crystalline peaks corresponding to aluminate and silicate [35]. In the Fig. 1h there are two peaks at 2θ = 8.4° and 21° which are significant peak of nano chitosan that is similar to pattern characterized in other researchers as well as is found as tendon" hydrated polymorph in the literature [36]. The significant characteristic peaks of synthetic allophane were

observed in the XRD pattern of chitosan-allophane nanocomposite (Fig. 1i). In addition, the intensity of the peaks for composite adsorbent was decreased that is due to hydrogen bounding of allophane and Nano chitosan [37].

SEM analysis

The SEM image of the synthetic allophane (Fig. 1j) is revealed that the morphology of allophane is spherical which is similar to published studies by other researchers [38]. The SEM images of synthesized nano chitosan are shown in Fig. 1k. As can be seen that the morphology of nano chitosan is rougher compared to allophane as well as is nano-sized that diameters of the aggregates are about 150 nm. The SEM images of chitosan-allophane nanocomposite is shown in Fig. 1l. As shown the morphology of nano composite has remained almost constant. Therefore, the morphology of the nanocomposite substrate has not changed after incorporation [34].

Study on Cr (VI)adsorption by adsorbents

The effect of contact time

In order to find the optimum adsorption time by chitosan-allophane nanocomposite, the different contact times in batch adsorption experiments on removal efficiency were investigated under different time values (time:2−60 min, pH:5, concetration:40 mg/l, 0.02 g of adsorbent), which were showed in Fig. 2a. As can be seen with increasing contact time, the removal efficiency enhanced because the time is adequate for interaction of ions and adsorbent which is physical adsorption [39]. The results have shown that when the time increases the removal efficiency remained stable and achieved the equilibration time. The findings of this study were in agreement with the literature reported previously for batch system [40]. The experimental data revealed that the percentage removal of Cr (VI) ions was 91.5% at 20 min of contact time as well as the reaction was nearly close to equilibrium after 60 minutes. So, the 20 min was considered as obtained contact time for saving time at removal of Cr (VI) ions.

The study of adsorbent dosage on Cr (VI) adsorption

For investigating properties of nano composite such as: efficiency, cost, environmental impact which are important to find the suitable amount of adsorbent in the removal of metal ions in the batch adsorption processes. Also, amounts of functional groups present on the surface is great importance that are sites for binding of ions. In this study, a series of experiments for investigating the influence of various adsorbent dosage (0.005−0.0325 g of adsorbent, concetration:60 mg/l, pH:5, time:20 min) on removal of Cr (VI) were performed that shown in Fig. 2b. The removal efficiency of Cr (VI) ions with increasing amount of adsorbent is increased because the surface area and adsorption sites were enhanced. Also, more adsorbent was added, the removal of Cr (VI) was not increased. Which is due to existence excess of adsorbent solution that is similar to other research [40, 41]. Therefore, the optimum mass of adsorbent was determined to be 0.03 g considering the cost, treatment efficiency, and other factors.

Effect of initial Cr (VI)concentration

The difference initial concentration of Cr (VI) ions (time:20 min, pH:5, concetration:20−100 mg/l, 0.02 g of adsorbent) is prepared to determine of performance of adsorbent which is revealed in Fig. 2c. The surface area, functional group on surface of adsorbent and concentration of desired analyte that adsorption on the adsorbent is important because the adsorption take place on the surface of adsorbent. So, the adsorbent with large surface area, the adsorption increases with the increasing Cr (VI) ion concentration that is to be adsorbed. As can be seen, the adsorption rate of Cr (VI) ions is fast in low initial concentration [42]. In the low initial concentration, the adsorption rate increased. This observation probably described that in the low initial concentration, the access to adsorption site on the surface of the nanocomposite is easy and convenient that is duo to the low amount of Cr (VI) ions in the solution. Thus, the adsorption of these ions happens on higher energy sites while the ion concentration of Cr (VI) ions in solution is increased, these sites are filled, and Cr (VI) ions uptake on lower energy sites. Therefore, the adsorption rate decreases remarkably [34, 40].

Effect of pH on adsorption of Cr (VI) ions

The effect pH is one of important factor that is affect on the adsorption process [43]. In order to determine performance adsorption of chromium ions in aqueous solution, the experiments were carried out in different pH (pH:1−10, time:20 min, concetration:60 mg/l, 0.02 g of adsorbent) by nanocomposite which is shown in Fig. 2d. There are three oxide forms of chromium that are included chromate ($[CrO_4]^{2-}$), dichromate ($[Cr_2O_7]^{2-}$), and perchromate ($[HCrO_4]^-$). The concertation of forms depends on pH that is highest at range 2−5 perchromate. As the pH increase from 5 to 11 deprotonation of perchromate takes place which is converted to chromate. The point of

zero charge of perchromate is at the pH 7. The concentration of dichromate is constant and stable through all the pH ranges [44]. As it can be seen the maximum removal of chromium take place in pH: 3 (Fig. 2d) In this pH both of the nano chitosan an allophane are protonated. Therefore, it is ascribed to strong attraction among the protonated surface of nanocomposite and the species of $HCrO_4^-$ in the solution by through electrostatic bond [45]. In the high-acidity solutions (lower of pH: 2) will increase the solubility of chitosan, thus the removal efficiency is reduced [41]. By increasing the pH to 8, deprotonation surface of nanocomposite is occurred which is reduced percentage of removal with a lower slope. This observation might have described through an anion exchange mechanism on allophane that hydroxyl anion of allophane replaces with chromate (Fig. 2e) When the pH was greater than 8 the anion exchange is reduced because of the OH^- ions of solution competing with chromate which results in a reduction in adsorption capacity which is similar results have been reported in the literature [42]. This study was not carried out under extreme alkaline conditions due to precipitation of chromium hydroxide.

Studying Cr (VI)adsorption reproducibility and stability of the adsorbents

The percentage of Cr (VI)adsorption, standard deviations and relative standard deviations (R.S.D.%) for four repeated experiments are calculated. The removal percentages are 98.6, 98.2, 97.1 and 96.8 in optimum conditions (concentration of Cr (VI) ions: 70 mg/l, pH: 3, amount of adsorbent:0.03 g, time: 20min). The obtained results show that efficiency of the adsorbents in removal of the Cr (VI)from aqueous samples is good, and are adsorbed more than 90% by chitosan-allophane nanocomposite. This process is reproducible and R.S.D.% is 0.88 as well as the stability of nanocomposite is investigated by FT-IR spectrum which is revealed that stability of adsorbent is appropriate after 3 times of absorption process (Fig. 2f) [46].

Isotherm of adsorption

The importance parameters of the initial and equilibrium concentration of the Cr (VI) are used in to determine the correlation between the adsorbed Cr (VI) concentration and concentration of the solution at equilibrium by isotherm models. The Langmuir and Freundlich models were investigated to explain the adsorption characteristics of the removal of Cr (VI)ions by nanocomposite adsorbent. In theory of Langmuir is assumed that the monolayer adsorption occurred on the adsorbent surface, the same active sites, there is not interaction between the adsorbed molecules, the limited adsorption capacity of adsorbent (q_{max}). The Freundlich model is based on the assumption that the adsorption of metal ions occurs on heterogeneous surface with multilayer adsorption and the adsorption increases with increase in concentration. The equation of Langmuir and Freundlich isotherm models are expressed as follows:

$C_e/q_e = (1/q_m) C_e + (1/q_m .b)$ (4)

$\ln q_e = (1/n) \ln C_e + \ln k_f$ (5)

where C_e is equilibrium concentration in solution, q_e (mg/g) is the Cr (VI)adsorption capacity at equilibrium concentration, b and q_m are Langmuir constants related to the energy of adsorption and adsorption capacity, respectively. The above parameters were computed from the intercept and linear gradient of the graphs of C_e/q_e and C_e (Fig. 3) [47]. Also, the values of Freundlich constant (K_F) and 1/n are obtained from the slope and the intercept of the plot of $\ln q_e$ vs. $\ln C_e$ (Fig. 3). The values of the isotherm parameters of Freundlich and Langmuir models, as well as the correlation coefficients for adsorbents were listed in Table 2. The Freundlich was fitted the experimental because the correlation coefficients of Freundlich (R^2) was 0.97 for synthetic chitosan-allophane nanocomposite.

The study of kinetics

In order to obtain design of adsorption systems the kinetic studies were used in the removal of Cr (VI) ions. The experimental studies were done to determine of optimum time for adsorption Cr (VI) ions on chitosan-allophane nanocomposite. The experiments are revealed that the adsorption is fast absorption until before 20 min and then slowly until it reaches equilibrium which it demonstrates that the Cr (VI) ions chemically interact with functional groups of chitosan-allophane nanocomposite. In the present work pseudo first-order and pseudo second-order have studied to find out the rate determining step of Cr (VI) adsorption chitosan-allophane nanocomposite. The kinetic equations of pseudo-first-order, pseudo-second-order and intra particle diffusion or particle diffusion models can be shown as follows, respectively:

$\ln (q_e - q_t) = \ln (q_e) - (k_1 \times t)$ (6)

$t/q_t = (1/(k_2 q_e^t)) + (t / q_e)$ (7)

$q_t = k_3 t^{0.5} + C$ (8)

where the Cr (VI) adsorption capacity at equilibrium concentration (mg/g) is shown with q_e, the amount of Cr (VI) adsorbed at time t (mg/g) is shown with q_t and the adsorption time (min) is shown with t. The K_1 and K_2 are represented for the pseudo-first-order rate constant adsorption (L/min), the pseudo-second-order rate constant adsorption (g/mg min), respectively. Also, C (mg/g) is the intercept related to the thickness of the boundary layer [48, 49]. The Fig. 3 show the parameters of adsorption kinetic models as well as the correlation coefficients (R^2) for adsorbents. The results of experiments carried out at 298 K are summarized in Table 2 which is revealed that the pseudo-second-order kinetic model was better fitted for chitosan-allophane nanocomposite in removal of Cr (VI) ions because the amount of R^2 is more than others. In addition, the experimental adsorption result (qe (exp)) was closer to qe (cal). Therefore, the pseudo-first-order model is not suitable to explain the adsorption kinetics of metal ions on adsorbent. So, the experimental data of the adsorption kinetics of metal ions are accurately supported by a pseudo-second-order model. Thus, these results suggests that the rate-limiting factor in the adsorption of Cr (VI) ions by chitosan-allophane nanocomposite is chemisorption involving the exchange of metal ions with the adsorbent, aligning well with the structural analysis conducted [48, 49].

Table 2
Isotherm and kinetic parameters for adsorption of Cr (VI) on chitosan-allophane nanocomposite.

Ion	Langmuir isotherm			Freundlich isotherm			Pseudo-first-order			Pseudo-second-order			
	b (L/mg)	q_m (mg/g)	R^2	K_f (L/g)	n (L/mg)	R^2	K_1 (L/min)	q_e (mg/g)	R^2	K_2 (g/mg.min)	q_e (mg/g)	R^2	q_e (mg/g)
Cr (VI)	0.34	142.85	0.92	42.9	2.8	0.97	3.01	175.91	0.77	0.001	125	0.94	112.17

Commerciality

In recent years, adsorption has been frequently employed for wastewater remediation, with aluminosilicate playing a Fundamental role in this process as a substitute for natural porous materials. Especially, synthetic allophane and nano chitosan have emerged as high surface area adsorbents used for the removal of Cr (VI) metal ions, proving to be cost-effective at $35.2 per ton. However, substantial quantities of the resulting adsorbent were required for the reactions. Our overarching goal has been to reduce the cost of catalyst production and enhance its environmental friendliness. Additionally, we aimed to minimize the amount of chitosan-allophane nanocomposite utilized in the adsorption process while ensuring efficient performance.

The comparison of the adsorption

The adsorption capacities of various adsorbents under different experimental conditions are presented in Table 3. In optimum conditions the adsorption capacity of chitosan-allophane nanocomposite was further compared with that of other adsorbents. Therefore, the results of the sorption capacity of chitosan-allophane nanocomposite are adequate for the adsorption of Cr (VI) from an aqueous solution. The high sorption capacity of chitosan-allophane nanocomposite attributed to more significant specific surface area and functional groups of chitosan-allophane nanocomposite [50, 51].

Table 3

Comparison of maximum adsorption capacity of prepared adsorbents for Cr (VI) adsorption compared with other adsorbents reported in the literature.

Adsorbent	Adsorption capacity (mg/g)	Reference
silica gel with 4-acetyl-3-hydroxyaniline	65	42
Natural Zeolite Coated with Magnetic Nanoparticles	43	52
Zn-NiF@PBC	84.46	53
CS-TiO$_2$	60	54
Chitosan/Zeolite film	17.28	55
Chitosan	35	55
Cross-Linked Magnetic Chitosan Beads	69.4	55
Prepared carbon with chestnut shells	33	56
chitosan-coated Bentonite	106.44	57
chitosan-allophane nanocomposite	112.17	This work

Conclusions

In briefly, the allophane was successfully synthesized under solvothermal condition and modified by nano chitosan. This adsorbent was characterized by (XRD), (SEM), (EDXA), (FT-IR) and (BET). The optimum conditions for removing Cr (VI) by chitosan-allophane nanocomposite was determined to be initial concentrations 70 mg/L; 0.03 g of adsorbent, pH:3 and contact time 20 min. The maximum capacity of adsorption of nanocomposite in optimum conditions for Cr (VI) was 112.17 mg/g. The present study reveals that the sorption capacity of mordenite is higher in compared to other adsorbents that is related to high surface area and functional groups of chitosan-allophane nanocomposite. The prepared adsorbents are low cost, non-toxic, and environmentally friendly that have the potential for Cr (VI) adsorption from aqueous media. The Langmuir and Freundlich's models were used to determine the adsorption isotherms that the Freundlich was fitted for synthetic nanocomposite. The kinetic analyses reveal that the adsorption process followed pseudo-second-order kinetics.

Declarations

Data availability

The datasets used and/or analyzed during the current study available from the corresponding author on reasonable request.

Author contributions

H.P.: Writing original draft. M.A.: Supervision, review and editing.

Competing interests

The authors declare no competing interests

Additional information.

Correspondence and requests for materials should be addressed to M.**A**

References

1. A. H. Mahvi, D. Balarak and E. Bazrafshan.Remarkable reusability of magnetic Fe3O4-graphene oxide composite: a highly effective adsorbent for Cr (VI) ions. Int J Environ Anal Chem. 103, 3501–3521 (2023).

2. M. Fazlzadeh, K. Rahmani, A. Zarei, H. Abdoallahzadeh, F. Nasiri and R. Khosravi.A novel green synthesis of zero valent iron nanoparticles (NZVI) using three plant extracts and their efficient application for removal of Cr(VI) from aqueous solutions. Adv Powder Technol 28, 122–130 (2017).

3. M. H. Dehghani, A. Zarei, A. Mesdaghinia, R. Nabizadeh, M. Alimohammadi and M. Afsharnia.Adsorption of Cr (VI) ions from aqueous systems using thermally sodium organo-bentonite biopolymer composite (TSOBC): response surface methodology, isotherm, kinetic and thermodynamic studies. Desalin. Water Treat. 85, 298–312 (2017).

4. F. Fu, L. Xie, B. Tang, Q. Wang and S. Jiang.Application of a novel strategy—Advanced Fenton-chemical precipitation to the treatment of strong stability chelated heavy metal containing wastewater. J. Chem. Eng. 189, 283–287 (2012).

5. J. Song, H. Oh, H. Kong and J. Jang.Polyrhodanine modified anodic aluminum oxide membrane for heavy metal ions removal. J. Hazard. Mater. 187, 311–317 (2011).

6. L. Tabandeh.Efficiency of a constructed wetland in controlling organic pollutants, nitrogen, and heavy metals from sewage. J. Chem. Pharm. Sci.

7. Y.-Y. Li, T.-T. Zhang, Z. Ning, J.-H. Chen and K. Hatfield.Characteristics and applications of sewage sludge biochar modified by ferrous sulfate for remediating Cr (VI)-contaminated soils. *Adv. Civ. Eng.* 2020, 1–10 (2020).

8. E. A. Ashour and M. A. Tony.Eco-friendly removal of hexavalent chromium from aqueous solution using natural clay mineral: activation and modification effects. Discover Applied Sciences. 2, 2042 (2020).

9. S. Salehi, S. Mandegarzad and M. Anbia.Preparation and characterization of metal organic framework-derived nanoporous carbons for highly efficient removal of vanadium from aqueous solution. J. Alloys Compd. 812, 152051 (2020).

10. B. Samiey, C.-H. Cheng and J. Wu.Organic-inorganic hybrid polymers as adsorbents for removal of heavy metal ions from solutions: a review. Materials. 7, 673–726 (2014).

11. A. Masoumi and M. Ghaemy.Removal of metal ions from water using nanohydrogel tragacanth gum-g-polyamidoxime: Isotherm and kinetic study. Carbohydr. Polym. 108, 206–215 (2014).

12. H. S. Altundogan, N. E. Arslan and F. Tumen.Copper removal from aqueous solutions by sugar beet pulp treated by NaOH and citric acid. J. Hazard. Mater. 149, 432–439 (2007).

13. R. Parfitt.Allophane in New Zealand-a review. Aust. J. Soil Res. 28, 343–360 (1990).

14. B. K. G. Theng, M. Russell, G. J. Churchman and R. L. Parfitt.Surface Properties of Allophane, Halloysite, and Imogolite. Clays Clay Miner. 30, 143–149 (1982).

15. L. Deng, P. Du, W. Yu, P. Yuan, F. Annabi-Bergaya, D. Liu and J. Zhou.Novel hierarchically porous allophane/diatomite nanocomposite for benzene adsorption. Appl. Clay Sci. 168, 155–163 (2019).

16. N. A. Limatahu and N. J. Baturante.Allophane of Gamalama Volcanic Soil Surface Modification Using Sulfuric Acid: Study of the Effect of Sulfuric Acid Concentration. Int. J. Appl. Chem. 15, 25–31 (2019).

17. R. Parfitt.Allophane and imogolite: role in soil biogeochemical processes. Clay Minerals. 44, 135–155 (2009).

18. F. Iyoda, S. Hayashi, S. Arakawa, B. John, M. Okamoto, H. Hayashi and G. Yuan.Synthesis and adsorption characteristics of hollow spherical allophane nano-particles. Appl. Clay Sci. 56, 77–83 (2012).

19. M. Rinaudo.Chitin and chitosan: Properties and applications. Prog. Polym. Sci. 31, 603–632 (2006).

20. F. Hoppe-Seiler.Chitin and chitosan. Ber Dtsch Chem Ges. 27, 3329–3331 (1994).

21. A. Domard and N. Cartier.Glucosamine oligomers: 4. Solid state-crystallization and sustained dissolution. Int. J. Biol. Macromol. 14, 100–106 (1992).

22. G. Crini and P.-M. Badot, *Sorption processes and pollution: conventional and non-conventional sorbents for pollutant removal from wastewaters*, Presses Univ. Franche-Comté, 2010.

23. P. Miretzky and A. F. Cirelli.Hg (II) removal from water by chitosan and chitosan derivatives: a review. J. Hazard. Mater. 167, 10–23 (2009).

24. Q. Gan, T. Wang, C. Cochrane and P. McCarron.Modulation of surface charge, particle size and morphological properties of chitosan–TPP nanoparticles intended for gene delivery. Colloids Surf. B. 44, 65–73 (2005).

25. P. Calvo, C. Remunan-Lopez, J. L. Vila-Jato and M. Alonso.Novel hydrophilic chitosan-polyethylene oxide nanoparticles as protein carriers. J. Appl. Polym. Sci. 63, 125–132 (1997).

26. X. X. TIAN and M. J. Groves.Formulation and biological activity of antineoplastic proteoglycans derived from Mycobacterium vaccae in chitosan nanoparticles. J. Pharm. Pharmacol. 51, 151–157 (1999).

27. H. Tokumitsu, H. Ichikawa, Y. Fukumori and L. H. Block.Preparation of gadopentetic acid-loaded chitosan microparticles for gadolinium neutron-capture therapy of cancer by a novel emulsion-droplet coalescence technique. Chem. Pharm. Bull. 47, 838–842 (1999).

28. S. Mitra, U. Gaur, P. Ghosh and A. Maitra.Tumour targeted delivery of encapsulated dextran–doxorubicin conjugate using chitosan nanoparticles as carrier. J. Control. Release. 74, 317–323 (2001).

29. M. H. Dehghani, A. Dehghan and A. Najafpoor.Removing Reactive Red 120 and 196 using chitosan/zeolite composite from aqueous solutions: Kinetics, isotherms, and process optimization. J. Ind. Eng. Chem. 51, 185–195 (2017).

30. W. W. Ngah, L. Teong, R. Toh and M. Hanafiah.Comparative study on adsorption and desorption of Cu (II) ions by three types of chitosan–zeolite composites. J. Chem. Eng. 223, 231–238 (2013).

31. P. I. Ravikovitch and A. V. Neimark.Characterization of nanoporous materials from adsorption and desorption isotherms. Colloids Surf. A. 187, 11–21 (2001).

32. H. Pazoki and M. Anbia.Synthesis of a microporous copper carboxylate metal organic framework as a new high capacity methane adsorbent. Polyhedron. 171, 108–111 (2019).

33. M. Doğan.Preparation of chitosan nanoparticles and characterization studies. Cumhur. Dent. J. 42 (2020).

34. F. Yazdi, M. Anbia and S. Salehi.Characterization of functionalized chitosan-clinoptilolite nanocomposites for nitrate removal from aqueous media. Int. J. Biol. Macromol. 130, 545–555 (2019).

35. A. Baldermann, A. C. Grießbacher, C. Baldermann, B. Purgstaller, I. Letofsky-Papst, S. Kaufhold and M. Dietzel.Removal of barium, cobalt, strontium, and zinc from solution by natural and synthetic allophane adsorbents. Geosciences. 8, 309 (2018).

36. E. Belamie, A. Domard and M. M. Giraud-Guille.Study of the solid-state hydrolysis of chitosan in presence of HCl. J Polym Sci A Polym Chem. 35, 3181–3191 (1997).

37. S. Arakawa, Y. Matsuura and M. Okamoto.Allophane–Pt nanocomposite: Synthesis and MO simulation. Appl. Clay Sci. 95, 191–196 (2014).

38. I. Cipta, N. A. Limatahu, N. St Hayatun, I. Kartini and Y. Arryanto.Effect of Allophane from Gamalama Volcanic Soil on Properties of BiOI-Allophane Composite. Asian J. Chem. 29, 1042 (2017).

39. D. Bhardwaj, M. Sharma, P. Sharma and R. Tomar.Synthesis and surfactant modification of clinoptilolite and montmorillonite for the removal of nitrate and preparation of slow release nitrogen fertilizer. J. Hazard. Mater. 227–228, 292–300 (2012).

40. T.-H. Pham, K.-M. Lee, M. S. Kim, J. Seo and C. Lee.La-modified ZSM-5 zeolite beads for enhancement in removal and recovery of phosphate. Microporous Mesoporous Mater. 279, 37–44 (2019).

41. M. Zhang, H. Zhang, D. Xu, L. Han, J. Zhang, L. Zhang, W. Wu and B. Tian.Removal of Phosphate from Aqueous Solution Using Zeolite Synthesized from Fly Ash by Alkaline Fusion Followed by Hydrothermal Treatment. Sep. Sci. Technol. 46, 2260–2274 (2011).

42. A. Bilgiç and A. Çimen.Removal of chromium (VI) from polluted wastewater by chemical modification of silica gel with 4-acetyl-3-hydroxyaniline. Rsc Advances. 9, 37403–37414 (2019).

43. V. S. Ruiz and C. Airoldi.Thermochemical data for n-alkylmonoamine intercalation into crystalline lamellar zirconium phenylphosphonate. Thermochim Acta. 420, 73–78 (2004).

44. S. A. S. Mohammed.Potential of surface complexation and redox modeling for chromium (VI) adsorption on local materials as liners for waste containment facilities. Turkish J. Eng. Environ. Sci. 37, 100–108 (2013).

45. J. Jia, Y. Liu and S. Sun.Preparation and characterization of chitosan/bentonite composites for Cr (VI) removal from aqueous solutions. Adsorp Sci Technol. 2021, 1–15 (2021).

46. M. Ahmadian and M. Anbia.Keggin-Type Heteropolyanions Immobilized on Phosphorus Slag Derived SiO2: Synthesis, Characterization, and Their Catalytic Oxidative Desulfurization Activity. Energy Fuels. 37, 16790–16804 (2023).

47. R. F. Spalding and M. E. Exner.Occurrence of Nitrate in Groundwater—A Review. J. Environ. Qual. 22, 392–402 (1993).

48. D. S. Powlson, T. M. Addiscott, N. Benjamin, K. G. Cassman, T. M. de Kok, H. van Grinsven, J.-L. L'Hirondel, A. A. Avery and C. van Kessel.When Does Nitrate Become a Risk for Humans? J. Environ. Qual. 37, 291–295 (2008).

49. L. Knobeloch, B. Salna, A. Hogan, J. Postle and H. Anderson.Blue babies and nitrate-contaminated well water. Environ. Health Perspect. 108, 675–678 (2000).

50. K. Wu, Y. Li, T. Liu, N. Zhang, M. Wang, S. Yang, W. Wang and P. Jin.Evaluation of the adsorption of ammonium-nitrogen and phosphate on a granular composite adsorbent derived from zeolite. Environ. Sci. Pollut. Res. 26, 17632–17643 (2019).

51. J.-R. Li, F.-K. Wang, H. Xiao, L. Xu and M.-L. Fu.Layered chalcogenide modified by Lanthanum, calcium and magnesium for the removal of phosphate from water. Colloids Surf. 560, 306–314 (2019).

52. M. Asanu, D. Beyene, A. Befekadu and W. Oueslati.Removal of hexavalent chromium from aqueous solutions using natural zeolite coated with magnetic nanoparticles: Optimization, kinetics, and equilibrium studies. *Adsorp Sci Technol.* 2022, 1–22 (2022).

53. M. Masuku, J. F. Nure, H. I. Atagana, N. Hlongwa and T. T. Nkambule.Advancing the development of nanocomposite adsorbent through zinc-doped nickel ferrite-pinecone biochar for removal of chromium (VI) from wastewater. Sci. Total Environ. 908, 168136 (2024).

54. Z. H. Mahmoud, A. Hamrouni, A. B. Kareem, M. A. Mostafa and A. H. Majeed.Synthesis and characterization of chitosan sheet modified by varied weight ratio of anatase (TiO2) nano mixture with Cr (VI) adsorbing. Kuwait J. Sci. (2023).

55. H. Moussout, H. Ahlafi, M. Aazza and C. El Akili.Performances of local chitosan and its nanocomposite 5% Bentonite/Chitosan in the removal of chromium ions (Cr (VI)) from wastewater. Int. J. Biol. Macromol. 108, 1063–1073 (2018).

56. L. Niazi, A. Lashanizadegan and H. Sharififard.Chestnut oak shells activated carbon: Preparation, characterization and application for Cr (VI) removal from dilute aqueous solutions. J. Clean. Prod. 185, 554–561 (2018).

57. T. Altun.Preparation and application of glutaraldehyde cross-linked chitosan coated bentonite clay capsules: Chromium (VI) removal from aqueous solution. J. Chil. Chem. Soc. 65, 4790–4797 (2020).
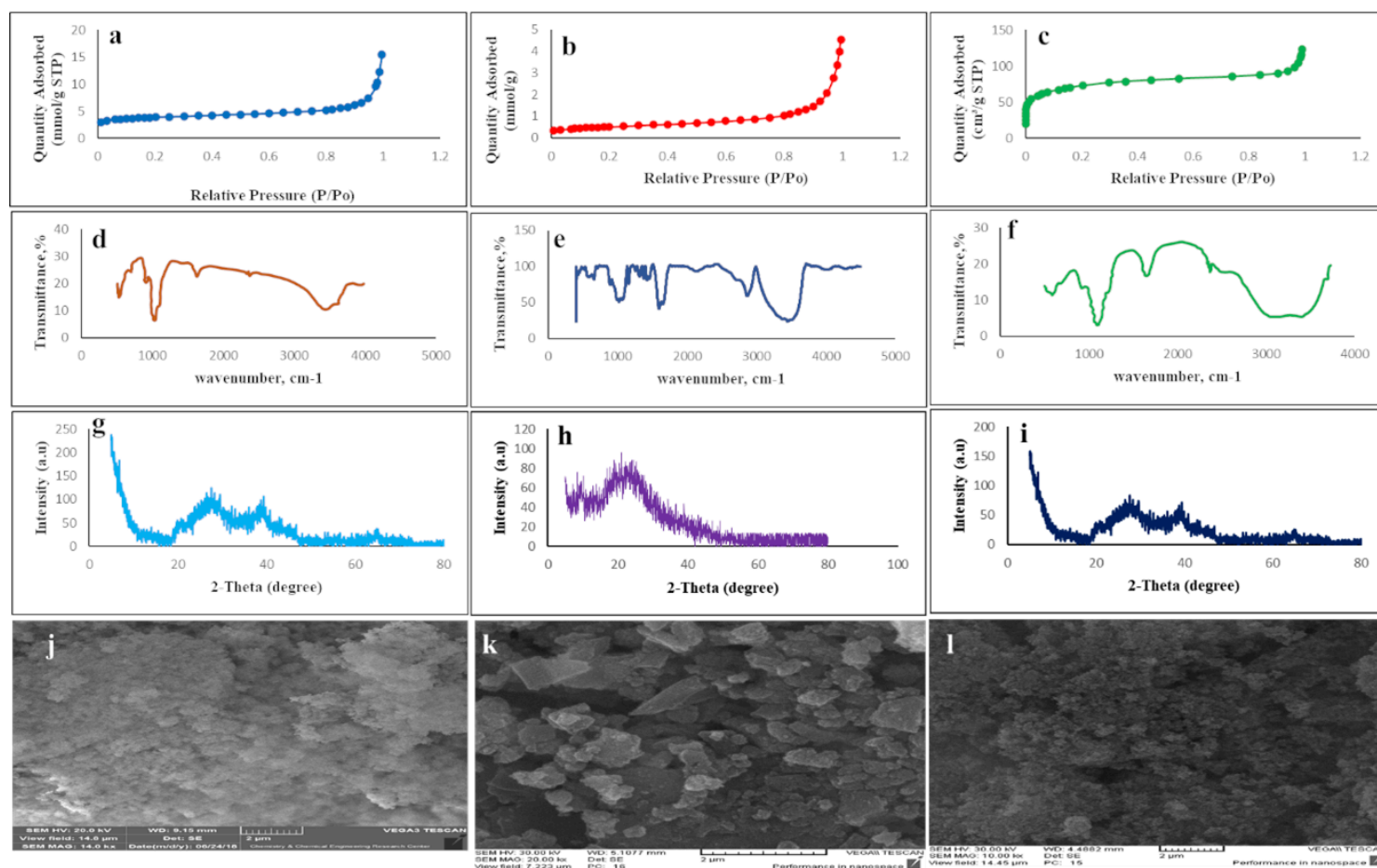
Figures

Figure 1

The N$_2$ adsorption-desorption (a-c), FT-IR spectrum (d-f), XRD pattern (g-i)), the SEM image (j-l) of synthetic allophane, Nano chitosan, chitosan-allophane nanocomposite, respectively.
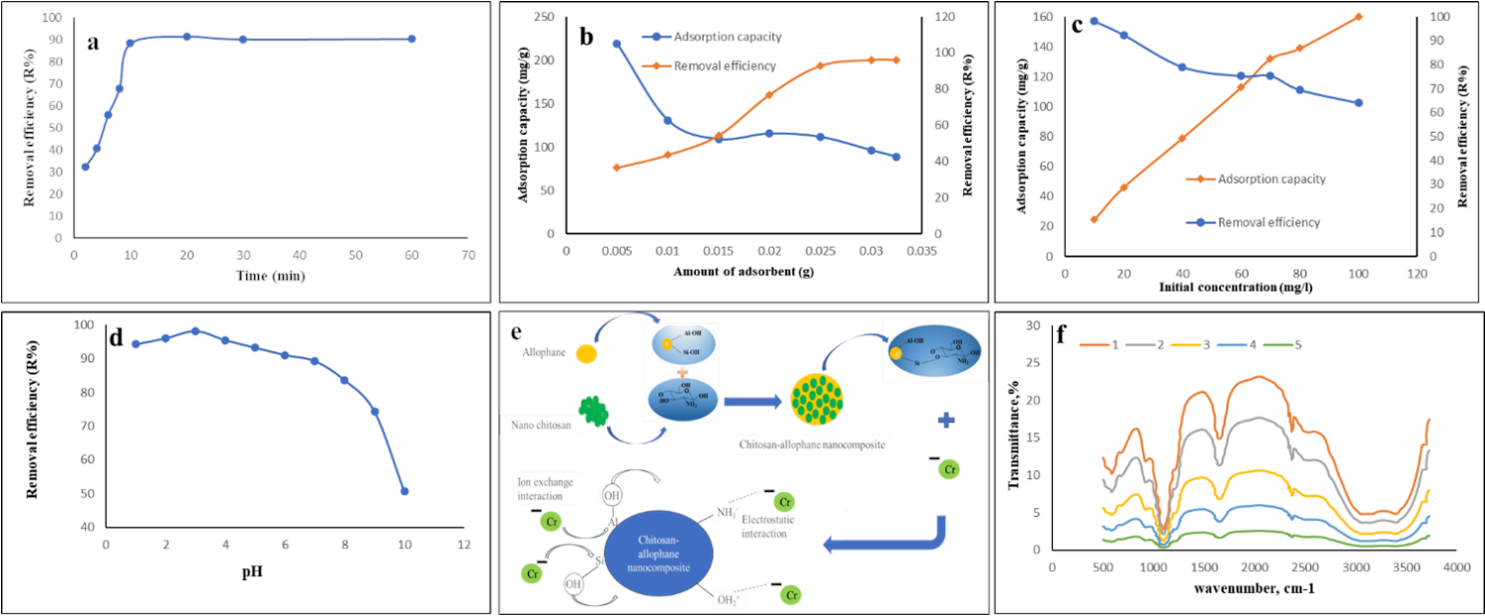

Figure 2

The effect of contact time (a), the study of adsorbent dosage on Cr (VI) adsorption (b), effect of initial Cr (VI)concentration (c), effect of pH on adsorption of Cr (VI) ions (d), synthesis and possible absorption mechanism of Cr (VI) (e), the study of stability (f) of the chitosan-allophane nanocomposite.
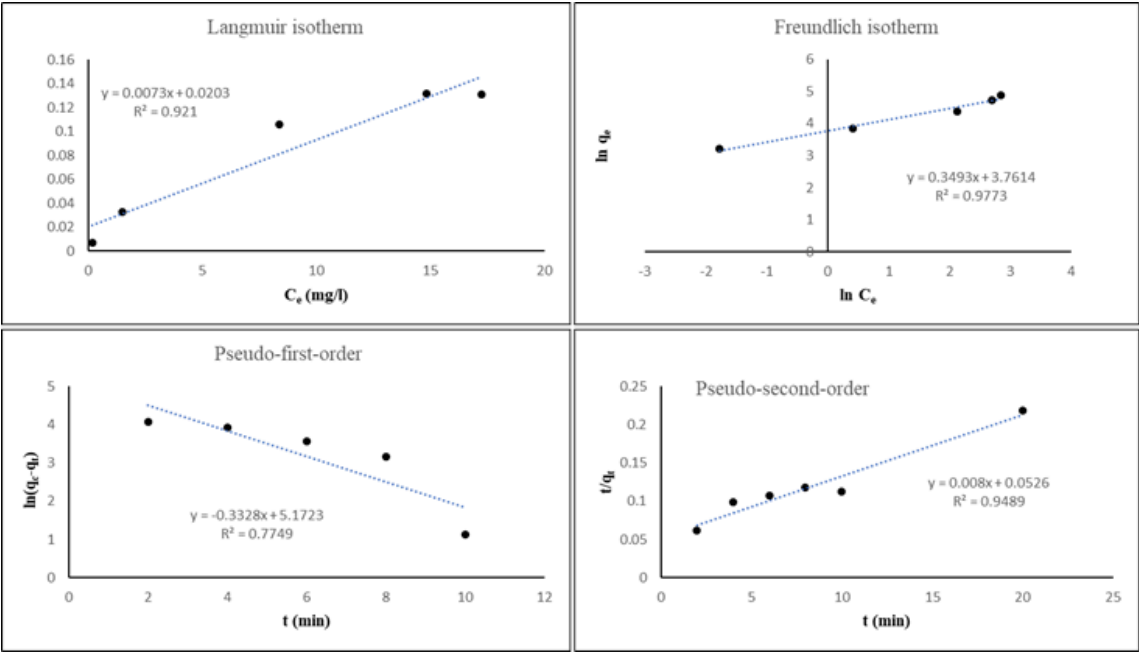

Figure 3

Linear Langmuir, Freundlich isotherm models and the pseudo-first-order, pseudo-second-order plots of Cr (VI) adsorption onto chitosan-allophane nanocomposite.